Available online at www.sciencedirect.com

ScienceDirect

journal homepage: www.elsevier.com/locate/he

First-principle investigation for the hydrogen storage properties of $NaXH_3$ (X= Mn, Fe, Co) perovskite type hydrides

Gokhan Surucu [a,b,*], *Abdullah Candan* [c], *Ayşenur Gencer* [d], *Mehmet Isik* [e]

[a] *Department of Electric and Energy, Ahi Evran University, Kirsehir, 40100, Turkey*
[b] *Department of Physics, Middle East Technical University, 06800, Ankara, Turkey*
[c] *Department of Machinery and Metal Technology, Ahi Evran University, Kirsehir, 40100, Turkey*
[d] *Department of Physics, Karamanoglu Mehmetbey University, Karaman, 70100, Turkey*
[e] *Department of Electrical and Electronics Engineering, Atilim University, 06836, Ankara, Turkey*

HIGHLIGHTS

- $NaXH_3$ (X = Mn, Fe, Co) Perovskite type hydrides have been investigated using Density Functional Theory (DFT).
- $NaXH_3$ (X = Mn, Fe, Co) Perovskite type hydrides are found to be energetically, mechanically and dynamically stable.
- Highest gravimetric hydrogen storage capacities are determined for $NaXH_3$.

ARTICLE INFO

Article history:
Received 4 August 2019
Received in revised form
21 September 2019
Accepted 25 September 2019
Available online 23 October 2019

Keywords:
Hydrogen storage
Perovskite type hydrides
First principle calculation
Band structure
Dynamic stability

ABSTRACT

In the present study, $NaXH_3$ (X = Mn, Fe, Co) perovskite type hydrides have been investigated by performing first-principles calculation. The results of the structural optimizations show that all these compounds have negative formation energy implying the thermodynamic stability and synthesisability. The mechanical stability of these compounds has been studied with the elastic constants. Moreover, the polycrystalline properties like bulk modulus, Poisson's ratio, etc. have been obtained using calculated elastic constants of interest compounds. The electronic properties have been studied and band structures have been drawn with the corresponding partial density of states. These plots indicated that $NaXH_3$ hydrides show metallic characteristics. The charge transfer characteristics in these compounds have been studied with the Bader partial charge analysis. The phonon dispersion curves and corresponding density of states indicated that $NaXH_3$ compounds are dynamically stable compounds. The investigation on hydrogen storage characteristics of $NaXH_3$ compounds resulted in hydrogen storage capacities of 3.74, 3.70 and 3.57 wt% for X = Mn, Fe and Co, respectively. The present study is the first investigation of $NaXH_3$ perovskite type hydrides as known up to date and may provide remarkable contribution to the future researches in hydrogen storage applications.

* *Corresponding author*. Department of Electric and Energy, Ahi Evran University, Kirsehir, 40100, Turkey.
E-mail addresses: g_surucu@yahoo.com, thesurucu@gmail.com, gsurucu@ahievran.edu.tr (G. Surucu).

https://doi.org/10.1016/j.ijhydene.2019.09.201
0360-3199/

Introduction

Hydrogen being the lightest fuel and most abundant element in the universe is thought as a non-toxic and cheap energy source for various applications. The remarkable properties of hydrogen enable to use it in energy storage fields [1]. Compounds used for energy storage purpose should satisfy some necessary conditions like high gravimetric and volumetric hydrogen storage capacities, reversibility, release of hydrogen at ambient conditions, good kinetics [2–4]. The compounds formulated as ABH_3 are known as perovskite type hydrides and have taken attention in recent years thanks to their potential technological applications especially hydrogen storage area [5–7]. The well-known two types of ABH_3 structures are formed as follows: (i) The A and B elements belong to monovalent alkali metal (like Li, Na, K) and divalent alkaline earth metal (like Be, Mg, Ca), respectively. (ii) The A element belongs to monovalent alkali or divalent metal while element B is a transition metal. The ideal crystalline structure of ABH_3 perovskite type hydrides is primitive cubic unit cell in which A and B are localized at corners and centers, respectively, and hydrogen atoms are positioned at the face-centered positions of the unit cell. In addition to these ABH_3-type structures, complex transition metal hydrides have been also investigated due to their potential as optical sensors, thermal energy and hydrogen storage materials [8–10].

ABH_3 type compounds having high gravimetric hydrogen storage capacities have been investigated due to their hydrogen storage potentials [5,6,11–13]. Among the ABH_3-type perovskite hydrides, the mostly studied perovskite type hydride is $NaMgH_3$ with 6 wt% gravimetric hydrogen storage capacity and 88 kg/m^3 volumetric hydrogen density [13–17]. Recent studies also pointed out that $NaMgH_3$ having superior hydrogen mobility may be a potential compound for future generation of electronic devices [18] and solar heat storage applications [19]. Although $NaMgH_3$ is one of the most favorable perovskite type hydride, investigations on other ABH_3-type perovskite hydrides have been also carried out to get information about their usage potential in relevant applications. The gravimetric hydrogen storage densities of members of this hydride group were generally obtained in between 1.2 and 6.0 wt% [7]. The aim of the present study is to examine $NaXH_3$ (X = Mn, Fe, Co) perovskite type hydrides by Density Functional Theory (DFT). In the literature there are limited number of papers on ABH_3 compounds in which A and B are group I and transition metal elements, respectively. Previously, $LiTH_3$ (*T* = Fe, Co, Ni and Cu) compounds were investigated using DFT study and it was shown that interest compounds are thermodynamically stable and synthesizable [20]. DFT study accomplished for $XNiH_3$ (X = Li, Na and K) perovskite hydrides presented structural, mechanical properties and hydrogen storage characteristics of compounds [12]. The gravimetric hydrogen storage densities of studied compounds were calculated as 3.38, 3.65 and 3.51 wt% for X: Li, Na and K, respectively. To the best of our knowledge, the present paper is the first detailed investigation on $NaXH_3$ (X = Mn, Fe, Co) perovskite type hydrides. The structural, electronic, elastic, dynamical properties and gravimetric hydrogen storage densities of studied compounds have been presented as a result of DFT calculations.

Computational details

The density functional theory (DFT) calculations have been performed using the Vienna Ab-initio Simulation Package (VASP) (version 535) [21,22]. The electron-ion interaction has been considered with the Projected Augmented Wave (PAW) method [23,24]. The electron-electron interaction has been studied using the Generalized Gradient Approximation (GGA) with Perdew-Burke-Ernzerhof (PBE) functional [25]. The cut-off energy has been taken as 600 eV and the gamma centered scheme [25] has been employed for the generation of k-points and it is obtained as 19 × 19 × 19 k-points for $CaFeH_3$ and $CaCoH_3$ and 18 × 18 × 18 k-points for $CaMnH_3$. The energy tolerance has been chosen as 10^{-5} eV per unit cell and the Hellman-Feynman forces has been converged with −0.02 eV/Å. The valence electron configuration has been considered as $2p^6 3s^1$ for Na atom, $3p^6 3d^5 4s^2$ for Mn atom, $3d^7 4s^1$ for Fe atom, $3d^8 4s^1$ for Co atom, and $1s^1$ for H atom. The stress-strain method as implemented in the VASP [21,22,26] has been used to obtain the elastic constants. VASP has been used to determine the Bader partial charge and the algorithm generated by Henkelman group [27] based on the atoms in the molecules [28] has been chosen to analyze the obtained results. The vibrational properties have been studied with the direct method [29] with the supercell approach that is generated using the PHONON software [30].

The gravimetric hydrogen storage capacities have been determined for $NaXH_3$ compounds. The hydrogen deposited per mass of a material is defined as the gravimetric storage capacity. Eq. (1) [31] could be used to determine the gravimetric storage capacity and m_H and m_{Host} are the molar masses of hydrogen and host material, respectively, and *H/M* is the hydrogen to material atom ratio.

$$C_{wt\%} = \left(\frac{\left(\frac{H}{M}\right) m_H}{m_{Host} + \left(\frac{H}{M}\right) m_H} \times 100 \right)\% \tag{1}$$

Results and discussion

Structural and hydrogen storage properties

$NaXH_3$ perovskite type hydrides belongs to 221 space group (*Pm*-3m) and their crystal structure is shown in Fig. 1. The optimized lattice parameters of cubic crystalline structures, volumes and densities have been listed in Table 1. These compounds have not been investigated as known up to now, so the obtained results could be compared with the studies in the future. As can be concluded from Table 1, $NaMnH_3$ has the highest lattice parameter (3.56 Å) while $NaCoH_3$ has the largest density (3.70 g/cm^3) among the studied hydrides. The formation enthalpies have been calculated using Eq. (2) in which $E_t(NaXH_3)$ is the total energy of $NaXH_3$ compounds, E(Na), E(X) and E(H) is the ground state energies for one Na

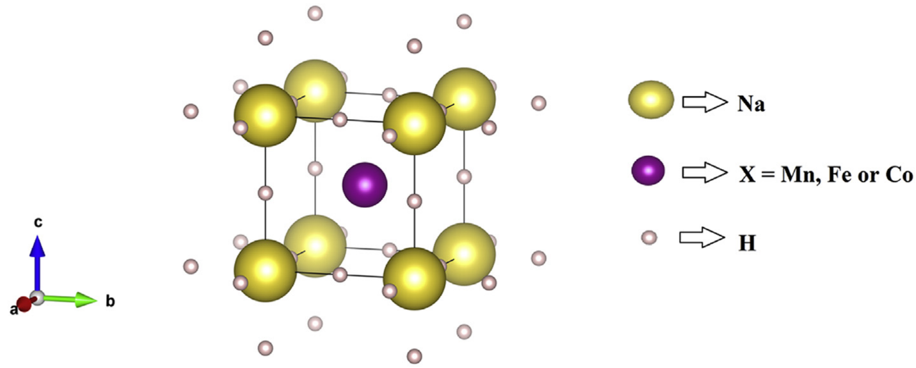

Fig. 1 – Crystal structure of $NaXH_3$ (X = Mn, Fe or Co) perovskite type hydrides.

Table 1 – The optimized lattice constant (*a* in Å), volume (*V* in $Å^3$), density (ρ in g/cm^3), formation enthalpy (ΔH_f in eV/atom), total magnetic moment (M_t in μ_B), and gravimetric hydrogen storage capacity ($C_{wt\%}$ in wt%) for $NaXH_3$ (X = Mn, Fe or Co).

Compound	a	V	ρ	ΔH_f	M_t (μ_B)	$C_{wt\%}$
$NaMnH_3$	3.56	44.99	2.99	−0.02	3.369	3.74
$NaFeH_3$	3.43	40.31	3.37	−0.09	1.839	3.70
$NaCoH_3$	3.37	38.12	3.70	−0.11	0.064	3.57

atom, one X atom and one H atom, respectively. All the studied compounds have negative formation enthalpy indicating the thermodynamic stability and synthesisability of the studied compounds as can be concluded from Table 1. The order of stability is as follows: $NaCoH_3$ (−0.11 eV/atom) > $NaFeH_3$ (−0.09 eV/atom) > $NaMnH_3$ (−0.02 eV/atom). $NaXH_3$ compounds have Mn, Fe or Co atom in its structure therefore the magnetic moment of these compounds should be studied. The obtained total magnetic moments of $NaXH_3$ compounds have also been listed in Table 1 and these moments are given in Bohr magneton. $NaMnH_3$ has the highest total magnetic moment (3.369 μ_B) among these compounds.

$$\Delta H_f = E_t(NaXH_3) - [E(Na) + E(X) + 3 * E(H)] \quad (2)$$

Some properties should be required for the hydrogen storage materials and the gravimetric hydrogen storage capacity was obtained for $NaXH_3$ compounds. As can be concluded from Table 1, $NaMnH_3$ has the largest gravimetric storage density (3.74 wt%) among the considered compounds. In the literature, $CaCoH_3$ compound which is thought as closer to studied $NaCoH_3$ compound was previously investigated for hydrogen storage applications [32]. The gravimetric hydrogen storage capacity of $CaCoH_3$ compound was reported as 2.9 wt% which is smaller than calculated 3.57 wt% of $NaCoH_3$.

Mechanical properties

The mechanical stability is essential for $NaXH_3$ compounds especially for their implementation in the mobile applications. For the mechanically stable compounds, the elastic constants (C_{ij}) must satisfy the Born stability criteria [33,34] that are given for the cubic crystals as

$$C_{11} - C_{12} > 0, \; C_{11} + 2C_{12} > 0, C_{11} > 0, \; C_{44} > 0 \quad (3)$$

The calculated elastic constants (C_{ij}) for $NaXH_3$ compounds have been reported in Table 2 where the sufficient constants are C_{11}, C_{12} and C_{44} for the cubic structures. It can be concluded from the values that $NaXH_3$ compounds are mechanically stable compounds with satisfying the Born stability criteria given in Eq. (3). So, these compounds are suitable for mobile applications. Moreover, Cauchy pressures (C_p) calculated from the relation C_{12}–C_{44} have also been listed in Table 2. The Cauchy pressure could be used to determine the ductile or brittle nature of a compound [35]. The negative Cauchy pressure value indicates the brittleness while the positive one indicates the ductility. $NaXH_3$ compounds have negative Cauchy pressures indicating that studied compounds are brittle materials. This brittleness property similar to $NaMgH_3$

Table 3 – The anisotropic index (A), longitudinal wave velocity (υ_l in m/s), transverse wave velocity (υ_t in m/s), average wave velocity (υ_m in m/s) and Debye temperature (θ_D in K) for $NaXH_3$ (X = Mn, Fe or Co).

Compound	A	υ_l	υ_t	υ_m	θ_D
$NaMnH_3$	0.84	6563	4183	4598	658.16
$NaFeH_3$	1.15	6720	4266	4691	696.57
$NaCoH_3$	0.93	7057	4327	4776	722.43

Table 2 – The calculated elastic constants (C_{ij} in GPa), Cauchy pressure (C_p in GPa), bulk modulus (*B* in GPa), shear modulus (*G* in GPa), Young's modulus (*E* in GPa), *B/G* ratio, *G/B* ratio and Poisson's ratio (ν) for $NaXH_3$ (X = Mn, Fe or Co).

Compound	C_{11}	C_{12}	C_{44}	C_P	B	G	E	B/G	G/B	ν
$NaMnH_3$	136.30	20.34	48.81	−28.47	58.99	52.29	121.10	1.13	0.89	0.16
$NaFeH_3$	145.67	32.89	64.94	−32.05	70.48	61.37	142.70	1.15	0.87	0.16
$NaCoH_3$	188.44	43.65	67.27	−23.62	91.91	69.28	166.10	1.33	0.75	0.20

[15] and $KMgH_3$ [36] perovskite type hydrides, is a drawback for $NaXH_3$ compounds that limits their applications in portable systems.

The polycrystalline properties could be determined with the calculated elastic constants. The bulk modulus (B), shear modulus (G), Young's modulus (E), *B*/*G*, *G*/*B* and Poisson's ratios for $NaXH_3$ compounds have been determined and listed in Table 2. The bulk modulus is a measure of the resistance to the volume change resulted from the application of a pressure. The shear modulus is the ratio of the shear stress to shear strain. The Young's modulus is related to the elasticity of a material and found from the ratio of stress to strain resulted from a uniaxial deformation. The reported bulk, shear and Young's moduli have been determined with the Voigt [37], Reuss [38] and Hill [39] approximations. The lowest extent of these moduli could be obtained with the Voigt approximation while the highest extent could be obtained with the Reuss approximation. The Hill approximation which is closer to the experimental values is the average of these results. The listed values for the bulk and shear moduli are the result of the Hill approximation. The remaining parameters could be obtained from the bulk and shear moduli. As can be revealed from the table, $NaCoH_3$ has the largest bulk, shear and Young's moduli within the considered compounds. Also, the $NaXH_3$ compounds have higher bulk, shear and Young's moduli than $NaMgH_3$ [15] and $KMgH_3$ [36]. So, the considered compounds are stiffer than $NaMgH_3$ and $KMgH_3$. *B*/*G* values are essential to reveal the ductility or brittleness of a compound and *B*/*G* ratio less than 1.75 implies the brittleness while *B*/*G* ratio larger than 1.75 indicate the ductility [40]. The $NaXH_3$ compounds have brittle nature (with B/G values as 1.13 for $NaMnH_3$, 1.15 for $NaFeH_3$ and 1.33 for $NaCoH_3$) and this result is consistent with results pointed out by the Cauchy pressure. The *G*/*B* ratio is useful for the investigation of the bonding type of a compound. The dominantly ionic bonding compounds have *G*/*B* ratio about 0.6 and G/B ratio is around 1.1 for the dominantly covalent bonding compounds [41]. The studied compounds have *G*/*B* ratio between the ionic and covalent bonding limits

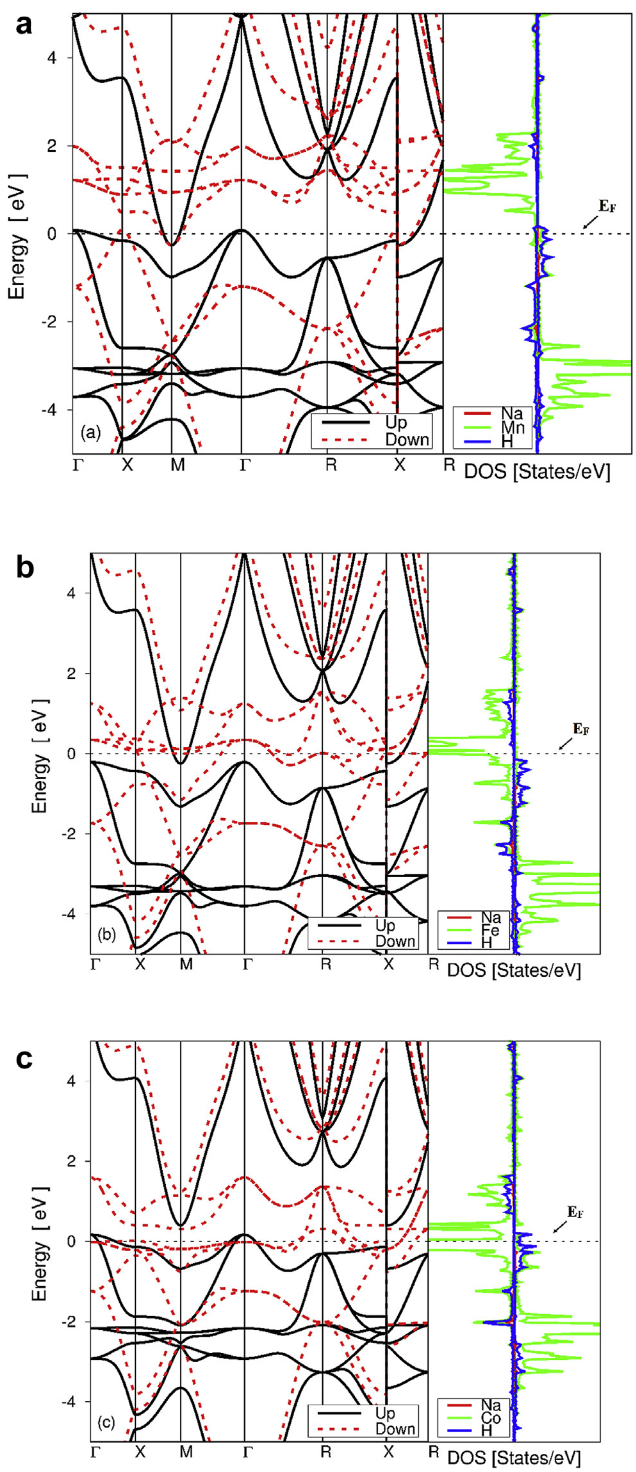

Fig. 2 – Electronic band structures with the partial density of states for (a) $NaMnH_3$, (b) $NaFeH_3$ and (c) $NaCoH_3$.

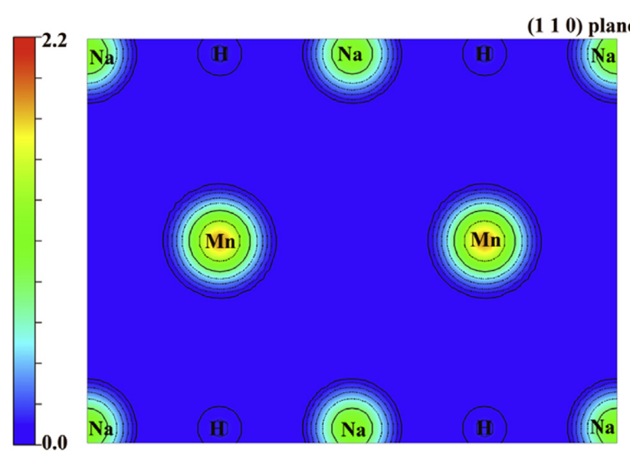

Fig. 3 – Electron-density distribution (in units of e) for $NaMnH_3$ in (110) plane.

Table 4 – Bader partial net charges for $NaXH_3$ (X = Mn, Fe or Co).

Bader Net Charge	$NaMnH_3$	$NaFeH_3$	$NaCoH_3$
Na	0.77	0.76	0.76
Mn/Fe/Co	0.70	0.89	0.68
H	−1.47	−1.65	−1.44

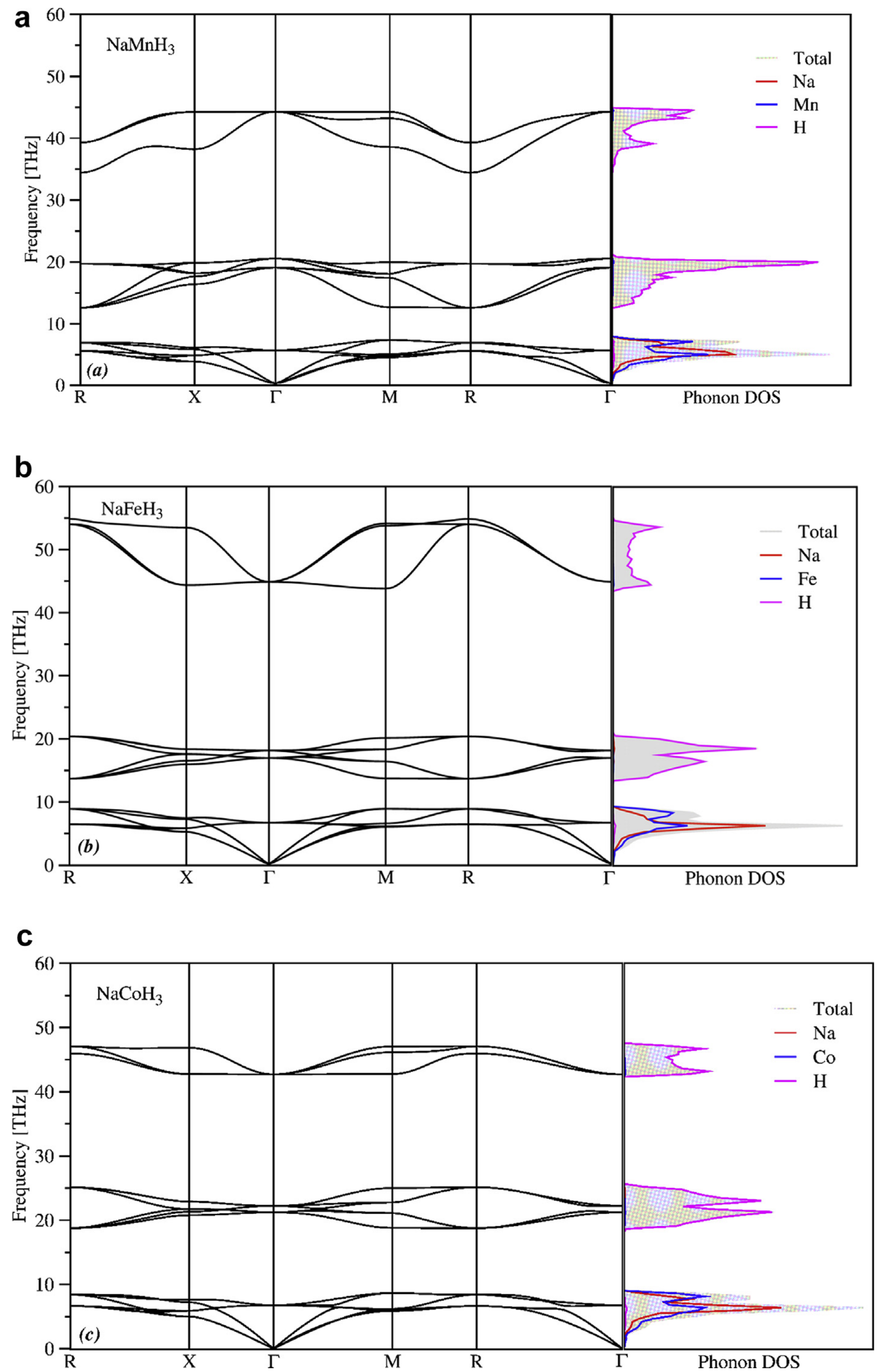

Fig. 4 – Phonon dispersion curves with the corresponding phonon density of states for (a) $NaMnH_3$, (b) $NaFeH_3$ and (c) $NaCoH_3$.

(0.89 for $NaMnH_3$, 0.87 for $NaFeH_3$ and 0.75 for $NaCoH_3$), so it can be established that they have both types of bonding. The last parameter in Table 2 is the Poisson's ratio (υ) that is the expansion in the perpendicular directions when a compression is applied or the contraction when a stretching is applied. It is also useful to get insight about the bonding characteristics of a material similar to G/B ratio. The dominantly ionic and covalent bonding materials have Poisson's ratio about 0.25 and 0.1, respectively [42]. The $NaXH_3$ compounds have Poisson's ratios between these limits presenting that interest compounds have both type of bonding consistent with indication of G/B values.

The anisotropic index, longitudinal wave velocity, transverse wave velocity, average wave velocity and Debye temperature have also been determined for $NaXH_3$ compounds using equations given in Refs. [43–45] and presented in Table

3. For the cubic crystals, the symmetry results with the equal anisotropic indexes A_1, A_2 and A_3. The isotropic materials have A value as one and the deviation from one results in the anisotropy. As can be concluded from Table 3, the most deviation for the A value belongs to $NaMnH_3$ which has the highest anisotropy among the considered compounds. The longitudinal, transverse and average wave velocities are also listed in the table. $NaCoH_3$ has the highest wave velocities among the $NaXH_3$ compounds. The Debye temperature is related to the melting temperature, specific heat, etc. If the Debye temperature is high, this means that related material has high thermal conductivity and high melting temperature. $NaCoH_3$ has the highest Debye temperature (722.43 K) among studied compounds as can be concluded from Table 3. Also, the calculated Debye temperatures are higher than the Debye temperatures of $NaMgH_3$ [15] and $KMgH_3$ [36]. Hence, $NaXH_3$ compounds have higher thermal conductivities and melting temperatures than $NaMgH_3$ and $KMgH_3$.

Electronic properties

Fig. 2 shows the band structures obtained along the high symmetry points in the first Brillouin zone as well as the corresponding density of states (DOS). Both of spin up and the spin down states have been drawn in the band structure plots. $NaXH_3$ compounds have metallic character since no forbidden gap exists between conduction and valence bands. Moreover, the partial density of states showed the contributions from the atoms in the compounds to the band structures. For $NaMnH_3$, the spin down states of Mn atom contribute more between 0.5 and 2.0 eV in the DOS plot and the spin up states of Mn atom contribute between −2.0 and −4.0 eV. For $NaFeH_3$, the spin down states of Fe atom contribute more between 0.5 and 2.0 eV in the DOS plot and also the spin up states of Fe atom contribute more between −2.5 and −4.5 eV. For $NaCoH_3$, the down states of Co atom contribute more between 2.0 and −1.0 eV in the DOS plot and also the spin up states of Co atom contribute more between −2.0 and −4.0 eV.

The electron-density distributions have been obtained and Fig. 3 shows the corresponding distribution for $NaMnH_3$ in (110) plane. As shown in the figure, $NaMnH_3$ has dominantly ionic bonding conforming the results pointed out by the Poisson's ratio and G/B ratio. Since $NaFeH_3$ and $NaCoH_3$ have similar distributions, they are not presented here due to space limitations. In addition to the electron-density distribution, the charge transfer in these compounds have been determined with the Bader partial charge. The positive (negative) Bader net charges indicate that the charge is delivered from (to) the atom. Table 4 lists the calculated Bader net charges. As can be concluded from the values in Table 4, the charge is delivered away from Na and X atoms and it is delivered to H atoms. In addition, the total charge is equal to zero for $NaXH_3$ compounds.

Lattice dynamical properties

The dynamical stabilities of $NaXH_3$ compounds have been investigated using direct method with the supercell approach. The supercells have been generated and the phonon frequencies have been calculated using PHONON software. Fig. 4 shows the phonon dispersion curves and corresponding phonon density of states (DOS) for $NaXH_3$ compounds. There are 15 phonon branches existing due to five atoms in the unit cell. Three of these branches are acoustic phonon modes and the remaining of them are optic branches. $NaXH_3$ compounds are dynamically stable due to no imaginary frequencies in the phonon dispersion curves. Also, Na and X atoms which are heavier than H give contributions to low frequencies while H atoms, the element having lowest mass in the compounds, contribute to high frequencies.

Conclusion

In this study, $NaXH_3$ (X = Mn, Fe or Co) have been investigated using DFT with VASP version 535. The optimized structures show that these compounds are synthesizable with thermodynamic stability. Also, the lattice constant of $NaMnH_3$ are lower than that of $NaCoH_3$. The calculated elastic constants have been revealed that these compounds are mechanically stable with satisfying the Born stable criteria. The determined elastic constants have been employed to obtain the polycrystalline properties and it has been found that $NaCoH_3$ has the largest bulk, shear and Young's moduli within the considered compounds. $NaXH_3$ compounds are found to be brittle and $NaXH_3$ compounds have both ionic bonding and covalent bonding. The obtained band structure plots reveal the metallic nature of these compounds. The charge is delivered away from the Na and X atoms while the charge is delivered to the H atoms obtained from the Bader partial charge analysis. These compounds are dynamically stable due to no imaginary frequencies in the phonon dispersion curves. The gravimetric storage densities are determined as 3.74, 3.70 and 3.57 wt% for $NaMnH_3$, $NaFeH_3$ and $NaCoH_3$, respectively. $NaXH_3$ compounds could be a promising materials for the hydrogen storage applications with both the thermodynamic, mechanic and dynamic stabilities and the high gravimetric hydrogen storage capacities.

Acknowledgments

This work was supported by the Ahi Evran University Research Project Unit under Project No PYO-KMY.4001.15.001.

REFERENCES

[1] Edwards PP, Kuznetsov VL, David WIF, Brandon NP. Hydrogen and fuel cells: towards a sustainable energy future. Energy Policy 2008;36:4356–62. https://doi.org/10.1016/J.ENPOL.2008.09.036.

[2] Walker G. Solid state hydrogen storage: materials and chemistry. Institute of Materials M. Woodhead Pub.; 2008.

[3] Schlapbach L, Züttel A. Hydrogen-storage materials for mobile applications. Nature 2001;414:353–8. https://doi.org/10.1038/35104634.

[4] Broom DP. Hydrogen storage materials: the characterisation of their storage properties. Springer; 2011.

[5] Rehmat B, Rafiq MA, Javed Y, Irshad Z, Ahmed N, Mirza SM. Elastic properties of perovskite-type hydrides $LiBeH_3$ and

$NaBeH_3$ for hydrogen storage. Int J Hydrogen Energy 2017;42:10038–46. https://doi.org/10.1016/J.IJHYDENE.2017.01.109.

[6] Reshak AH. $NaMgH_3$ a perovskite-type hydride as advanced hydrogen storage systems: electronic structure features. Int J Hydrogen Energy 2015;40:16383–90. https://doi.org/10.1016/J.IJHYDENE.2015.10.030.

[7] Ikeda K, Sato T, Orimo S. Perovskite-type hydrides – synthesis, structures and properties. Int J Mater Res 2008;99:471–9. https://doi.org/10.3139/146.101671.

[8] Schouwink P, Ley MB, Tissot A, Hagemann H, Jensen TR, Smrčok Ľ, et al. Structure and properties of complex hydride perovskite materials. Nat Commun 2014;5:5706. https://doi.org/10.1038/ncomms6706.

[9] Humphries TD, Sheppard DA, Li G, Rowles MR, Paskevicius M, Matsuo M, et al. Complex hydrides as thermal energy storage materials: characterisation and thermal decomposition of $Na_2Mg_2NiH_6$. J Mater Chem 2018;6:9099–108. https://doi.org/10.1039/C8TA00822A.

[10] Møller K, Sheppard D, Ravnsbæk D, Buckley C, Akiba E, Li H-W, et al. Complex metal hydrides for hydrogen, thermal and electrochemical energy storage. Energies 2017;10:1645. https://doi.org/10.3390/en10101645.

[11] Candan A, Kurban M. Electronic structure, elastic and phonon properties of perovskite-type hydrides $MgXH_3$ (X=Fe, Co) for hydrogen storage. Solid State Commun 2018;281:38–43. https://doi.org/10.1016/J.SSC.2018.07.004.

[12] Gencer A, Surucu G. Investigation of structural, electronic and lattice dynamical properties of $XNiH_3$ (X = Li, Na and K) perovskite type hydrides and their hydrogen storage applications. Int J Hydrogen Energy 2019;44:15173–82. https://doi.org/10.1016/J.IJHYDENE.2019.04.097.

[13] Tao S, Wang Z, Wan Z, Deng J, Zhou H, Yao Q. Enhancing the dehydriding properties of perovskite-type $NaMgH_3$ by introducing potassium as dopant. Int J Hydrogen Energy 2017;42:3716–22. https://doi.org/10.1016/J.IJHYDENE.2016.07.174.

[14] Ikeda K, Kogure Y, Nakamori Y, Orimo S. Reversible hydriding and dehydriding reactions of perovskite-type hydride $NaMgH_3$. Scr Mater 2005;53:319–22. https://doi.org/10.1016/J.SCRIPTAMAT.2005.04.010.

[15] Bouhadda Y, Bououdina M, Fenineche N, Boudouma Y. Elastic properties of perovskite-type hydride $NaMgH_3$ for hydrogen storage. Int J Hydrogen Energy 2013;38:1484–9. https://doi.org/10.1016/J.IJHYDENE.2012.11.047.

[16] Ikeda K, Kato S, Shinzato Y, Okuda N, Nakamori Y, Kitano A, et al. Thermodynamical stability and electronic structure of a perovskite-type hydride. $NaMgH_3$. J Alloys Compd 2007;446–447:162–5. https://doi.org/10.1016/J.JALLCOM.2007.03.093.

[17] Wu H, Zhou W, Udovic TJ, Rush JJ, Yildirim T. Crystal chemistry of perovskite-type hydride $NaMgH_3$: implications for hydrogen storage. Chem Mater 2008;20:2335–42. https://doi.org/10.1021/cm703356v.

[18] Pottmaier D, Pinatel ER, Vitillo JG, Garroni S, Orlova M, Baró MD, et al. Structure and thermodynamic properties of the $NaMgH_3$ perovskite: a comprehensive study. Chem Mater 2011;23:2317–26. https://doi.org/10.1021/cm103204p.

[19] Sheppard DA, Paskevicius M, Buckley CE. Thermodynamics of hydrogen desorption from $NaMgH_3$ and its application as a solar heat storage medium. Chem Mater 2011;23:4298–300. https://doi.org/10.1021/cm202056s.

[20] Takagi S, Saitoh H, Endo N, Sato R, Ikeshoji T, Matsuo M, et al. Density-functional study of perovskite-type hydride $LiNiH_3$ and its synthesis: mechanism for formation of metallic perovskite. Phys Rev B 2013;87:125134. https://doi.org/10.1103/PhysRevB.87.125134.

[21] Kresse G, Furthmüller J. Efficient iterative schemes for *ab initio* total-energy calculations using a plane-wave basis set. Phys Rev B 1996;54:11169–86. https://doi.org/10.1103/PhysRevB.54.11169.

[22] Kresse G, Furthmüller J. Efficiency of ab-initio total energy calculations for metals and semiconductors using a plane-wave basis set. Comput Mater Sci 1996;6:15–50. https://doi.org/10.1016/0927-0256(96)00008-0.

[23] Kresse G, Joubert D. From ultrasoft pseudopotentials to the projector augmented-wave method. Phys Rev B 1999;59:1758–75. https://doi.org/10.1103/PhysRevB.59.1758.

[24] Blöchl PE. Projector augmented-wave method. Phys Rev B 1994;50:17953–79. https://doi.org/10.1103/PhysRevB.50.17953.

[25] Perdew JP, Burke K, Ernzerhof M. Generalized gradient approximation made simple. Phys Rev Lett 1996;77:3865–8. https://doi.org/10.1103/PhysRevLett.77.3865.

[26] Le Page Y, Saxe P. Symmetry-general least-squares extraction of elastic data for strained materials from *ab initio* calculations of stress. Phys Rev B 2002;65:104104. https://doi.org/10.1103/PhysRevB.65.104104.

[27] Tang W, Sanville E, Henkelman G. A grid-based Bader analysis algorithm without lattice bias. J Phys Condens Matter 2009;21:084204. https://doi.org/10.1088/0953-8984/21/8/084204.

[28] Bader RFW. Atoms in molecules: a quantum theory. Clarendon Press; 1990.

[29] Krzysztof Parlinski. PHONON Software. n.d, http://wolf.ifj.edu.pl/phonon/index.html. [Accessed 27 June 2019].

[30] Parlinski K, Li ZQ, Kawazoe Y. First-principles determination of the soft mode in cubic ZrO_2. Phys Rev Lett 1997;78:4063–6. https://doi.org/10.1103/PhysRevLett.78.4063.

[31] Baysal MB, Surucu G, Deligoz E, Ozısık H. The effect of hydrogen on the electronic, mechanical and phonon properties of $LaMgNi_4$ and its hydrides for hydrogen storage applications. Int J Hydrogen Energy 2018;43:23397–408. https://doi.org/10.1016/J.IJHYDENE.2018.10.183.

[32] Ikeda K, Kato S, Ohoyama K, Nakamori Y, Takeshita HT, Orimo S. Formation of perovskite-type hydrides and thermal desorption processes in Ca–T–H (T = 3d transition metals). Scr Mater 2006;55:827–30. https://doi.org/10.1016/J.SCRIPTAMAT.2006.07.016.

[33] Born M. On the stability of crystal lattices. I. Math Proc Camb Philos Soc 1940;36:160–72. https://doi.org/10.1017/S0305004100017138.

[34] Mouhat F, Coudert F-X. Necessary and sufficient elastic stability conditions in various crystal systems. Phys Rev B 2014;90:224104. https://doi.org/10.1103/PhysRevB.90.224104.

[35] Pettifor DG. Theoretical predictions of structure and related properties of intermetallics. Mater Sci Technol 1992;8:345–9. https://doi.org/10.1179/mst.1992.8.4.345.

[36] Ghebouli MA, Ghebouli B, Bouhemadou A, Fatmi M, Bin-Omran S. Structural, elastic, electronic, optical and thermodynamic properties of $KMgH_3$. Solid State Sci 2011;13:647–52. https://doi.org/10.1016/J.SOLIDSTATESCIENCES.2010.11.046.

[37] Voigt W. Lehrbuch der Kristallphysik. Wiesbaden: Vieweg+Teubner Verlag; 1966. https://doi.org/10.1007/978-3-663-15884-4.

[38] Reuss A. Berechnung der Fließgrenze von Mischkristallen auf Grund der Plastizitätsbedingung für Einkristalle. ZAMM – Zeitschrift Für Angew Math Und Mech 1929;9:49–58. https://doi.org/10.1002/zamm.19290090104.

[39] Hill R. The elastic behaviour of a crystalline aggregate. Proc Phys Soc Sect A 1952;65:349–54. https://doi.org/10.1088/0370-1298/65/5/307.

[40] Surucu G, Colakoglu K, Deligoz E, Korozlu N. First-principles study on the MAX phases Ti $_{n+1}GaN_n$ (n = 1,2, and 3). J

Electron Mater 2016;45:4256–64. https://doi.org/10.1007/s11664-016-4607-1.

[41] Gencer A, Surucu G. Electronic and lattice dynamical properties of Ti_2SiB MAX phase. Mater Res Express 2018;5:076303. https://doi.org/10.1088/2053-1591/aace7f.

[42] Surucu G. Investigation of structural, electronic, anisotropic elastic, and lattice dynamical properties of MAX phases borides: an Ab-initio study on hypothetical M_2AB (M = Ti, Zr, Hf; A = Al, Ga, In) compounds. Mater Chem Phys 2018;203:106–17. https://doi.org/10.1016/J.MATCHEMPHYS.2017.09.050.

[43] Schreiber E, Anderson OL, Soga N. Elastic constants and their measurement. McGraw-Hill; 1974.

[44] Miao N, Sa B, Zhou J, Sun Z. Theoretical investigation on the transition-metal borides with Ta_3B_4-type structure: a class of hard and refractory materials. Comput Mater Sci 2011;50:1559–66. https://doi.org/10.1016/J.COMMATSCI.2010.12.015.

[45] Anderson OL. A simplified method for calculating the debye temperature from elastic constants. J Phys Chem Solids 1963;24:909–17. https://doi.org/10.1016/0022-3697(63)90067-2.